

Article

# A Portable and Low-Cost Triboelectric Nanogenerator for Wheelchair Table Tennis Monitoring

Xiaorui Zhu <sup>1,2</sup> , Mengqi Zhang <sup>3</sup>, Xiaodong Wang <sup>3</sup>, Changjun Jia <sup>3,\*</sup> and Yingqiu Zhang <sup>1,\*</sup><sup>1</sup> Sports Coaching College, Beijing Sport University, Beijing 100084, China<sup>2</sup> Physical Education College, Shanxi University, Taiyuan 030006, China<sup>3</sup> Physical Education Department, Northeastern University, Shenyang 110819, China

\* Correspondence: 2071367@stu.neu.edu.cn (C.J.); 13810190222@163.com (Y.Z.)

**Abstract:** With progress in fifth-generation techniques, more advanced techniques are available for disabled people. Disability table tennis has also benefited from the new technology. In this paper, a portable and low-cost triboelectric nanogenerator for wheelchair table tennis monitoring systems is proposed. It was applied for wheelchair table tennis athletes' monitoring. The portable and low-cost triboelectric nanogenerator consists of Kapton, polyurethane triboelectric films, and a foam supporting layer. The materials have flexible and low-cost characteristics. Therefore, the device has no influence on exercise performance. Due to triboelectric and electrostatic induction, the portable and low-cost triboelectric nanogenerator can convert biomechanical signals into electric signals. The electric signal is used as a sensing signal and is transformed in a computer by an Analog-to-Digital acquisition module. The coach acquires motion information in real time from a terminal device regarding force, exercise amplitude, and stability of the athlete. Meanwhile, the electric signal provides also sustainable energy for the microelectronic device. It can light 20 LEDs easily and power a calculator and a watch. This portable and low-cost self-powered triboelectric nanogenerator offers a new approach to the field of motion monitoring for disabled people.

**Keywords:** nanogenerator; sensing; sports monitoring; wheelchair table tennis



**Citation:** Zhu, X.; Zhang, M.; Wang, X.; Jia, C.; Zhang, Y. A Portable and Low-Cost Triboelectric Nanogenerator for Wheelchair Table Tennis Monitoring. *Electronics* **2022**, *11*, 4189. <https://doi.org/10.3390/electronics11244189>

Academic Editor: Yue Wu

Received: 14 November 2022

Accepted: 14 December 2022

Published: 15 December 2022

**Publisher's Note:** MDPI stays neutral with regard to jurisdictional claims in published maps and institutional affiliations.



**Copyright:** © 2022 by the authors. Licensee MDPI, Basel, Switzerland. This article is an open access article distributed under the terms and conditions of the Creative Commons Attribution (CC BY) license (<https://creativecommons.org/licenses/by/4.0/>).

## 1. Introduction

The Tokyo Summer Paralympic Games and Beijing Winter Paralympic Games gave the opportunity to the disabled to show their courage and competitive spirit [1]. The society came to realize the power of sports in changing the lives of people with disabilities [2]. Wheelchair table tennis is one of the popular sports in the Paralympic Games [3]. Wheelchair table tennis differs from table tennis in that wheelchair table tennis players need to maintain greater balance when batting [4]. Real-time monitoring of athletes' balance while playing can provide data to support athletes' technical improvement. The traditional sports monitoring equipment is bulky and inflexible [5]; therefore, it is difficult to monitor the movement of wheelchair table tennis players in real time. In addition, the traditional monitoring equipment needs an external battery. Frequent battery replacement will pollute the environment. It is thus necessary to find a kind of portable, multifunctional, and safe sensing equipment for monitoring wheelchair table tennis.

The triboelectric nanogenerator (TENG) was first invented by Zhonglin Wang and his colleagues [6–10]. Based on the coupling effect of triboelectric and electrostatic induction, the TENG can output external mechanical stimuli as electrical signals [11,12]. TENG-based sensors work without an external power supply or batteries [13–18]. The TENG provides a new prospect for motion monitoring based on its own advantages of portability and environmental protection [19–36]. In addition, due to its characteristics of high voltage and low current, the TENG can be used for human body monitoring [37,38]. TENG technology can be used for motion monitoring to meet the need for flexibility and convenience in

wheelchair table tennis. An intelligent training aid system consisting of the TENG allows athletes to perform technically during motion monitoring independent of the monitoring equipment. The four operating modes of the TENG are the vertical contact-separation (CS) mode, the lateral sliding (LS) mode, the single-electrode (SE) mode, and the independent triboelectric-layer (FT) mode [39–41]. The main TENG used for human activity monitoring in current research is the LS-TENG [42–44], which provides energy for the monitoring equipment through the reciprocating motion of the human body. However, constant rubbing leads to a high loss of equipment [45]. This mode of operation, which relies on reciprocal motion to provide energy, is not suitable for monitoring changes in an athlete's trunk center of gravity. Therefore, there is still a need to design a flexible TENG suitable for the long-term continuous monitoring of trunk stability to meet the needs of wheelchair table tennis monitoring.

In this paper, a portable and low-cost triboelectric nanogenerator (PL-TENG) was designed. The PL-TENG is made of flexible PU and Kapton as a triboelectric layer, foam glue as a substrate, and copper foil as the conductive electrode. Its production process is simple, with a low material cost, and easy to achieve. It can be used as an energy harvesting implement to supply power to small electronic devices without causing environmental pollution. In practical applications, the PL-TENG can be used for monitoring wheelchair table tennis sports without the support of an external power source. The PL-TENG is easily fixed to the athlete's wheelchair by means of flexible tape. Because of its small size, the PL-TENG interferes little with the athlete. Based on this, the PL-TENG allows miniature electronic devices to achieve wireless data transmission and real-time monitoring of movement. The intuitive analysis of biomechanical movements by the sensing equipment with the PL-TENG promotes the application of small electronic sensing devices, led by the TENG, in the field of sports monitoring. The development of the PL-TENG intelligent training aid system opens new directions in sports monitoring for people with disabilities.

## 2. Materials and Methods

### 2.1. Materials

The polyurethane (PU) film and foam glue were purchased from Dongguan Jinda Plastic Insulation Material Shop (Dongguan, China). Kapton was purchased from Beijing Lancheng Feifan Technology Co., LTD. (Beijing, China). Enameled wire was purchased from Wuhu Eriter Electromechanical Equipment Co., LTD. (Wuhu, China). The one-sided matte copper foil was purchased from Taizhou Beiling Strength Store (Taizhou, China).

### 2.2. Methods

Firstly, Kapton and PU were cut into two rectangles with a length of 8.5 cm and a width of 4 cm. Secondly, the foam glue was cut into a rectangular frame according to the size of the triboelectric material. The frame was 8.5 cm long and 4 cm wide. The foam glue was tightly bonded between the Kapton and the PU layers as a support layer. The copper foil was cut into two rectangles of length and width of 7 cm and 2.8 cm and tightly bonded to the Kapton and PU surfaces [46]. Finally, the Kapton and PU layers of the same size were glued on the exposed surface of the copper foil as the substrate. Figure 1b shows the shape of the constituent materials and the bonding position. The material is easy to obtain, and its price is low. Compared with the traditional monitoring equipment, this equipment is less expensive and can be widely used in human motion monitoring.

### 2.3. Characterization and Measurements

The PL-TENG was fixed on the stepping motor frame with adhesive tape. The linear motor was set to output motion with different amplitudes and frequencies that simulated human motion through the control system. The PL-TENG generated triboelectric signals through repeated and periodic impacts of the stepping motor. An oscilloscope (sto1102c, Shenzhen, China) was used to collect the electrical signals generated by the PL-TENG located on the human body or stepping motor. The STM32 was adopted as the master

control, and the hardware acquisition frequency was 200 Hz. The model of Bluetooth was HC-05.

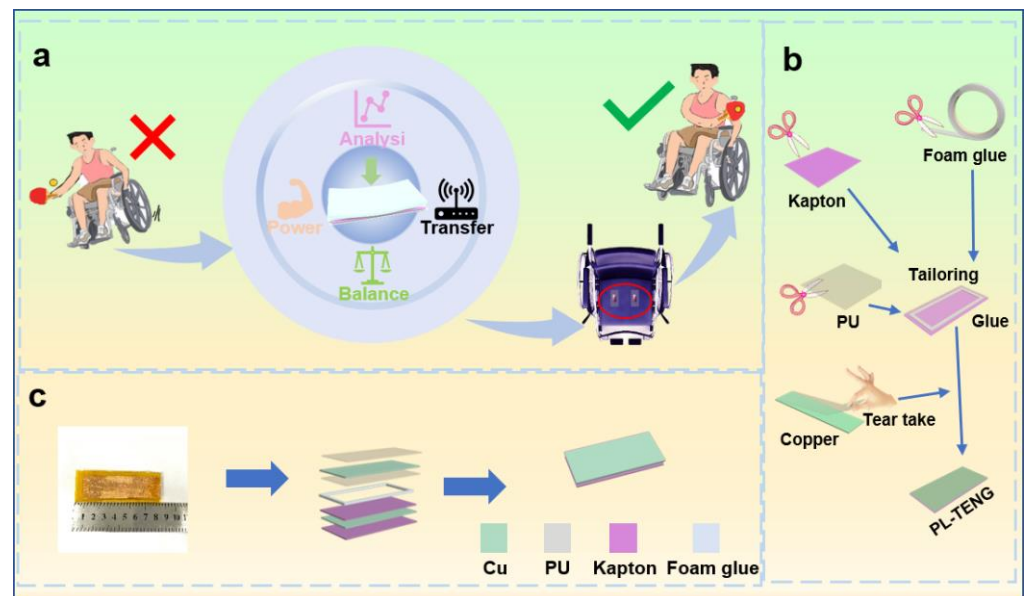


**Figure 1.** Experimental design for wheelchair table tennis balance monitoring and composition of the PL-TENG. (a) Working scenario of the PL-TENG. (b) Fabrication process of the PL-TENG. (c) Structure and 3D simulation of the PL-TENG.

### 3. Results and Discussion

The ability to control the body balance is one of the most important factors in wheelchair table tennis. The PL-TENG designed in this study can be mainly used for the monitoring of wheelchair table tennis. It can transmit posture balance information of athletes in real time. The legs of the player cannot transfer the body, in contrast to what occurs with table tennis players. In wheelchair table tennis, the transfer of the center of gravity of the body depends on the trunk strength transfer. The PL-TENG-L and PL-TENG-R were installed on the wheelchair seat (Figure S1). An athlete's center of gravity changes with the movement of his body. Different actions exert unequal pressures on the PL-TENG-L and PL-TENG-R. The mechanical stimulation generated by the pressure change acts on the PL-TENG. Different movements lead the PL-TENG to produce different electrical signals. Coaches and athletes can improve the movement technique according to the signals transmitted by the PL-TENG. Figure 1 shows the production and application of the PL-TENG. As shown in Figure 1a, the PL-TENG can monitor the movement techniques and movement changes of athletes in real time. The production process of the PL-TENG is shown in Figure 1b. The physical diagram and 3d simulation structure of the PL-TENG are shown in Figure 1c.

Figure 2a shows the working mechanism of the PL-TENG in CS mode. In the initial state, the two triboelectric layers come in contact with an external force. The positive and the negative triboelectric layers generate equal and opposite charges; therefore, the charges do not transfer (state i). When the external force disappears or decreases, the two triboelectric layers gradually separate, and the electrons are repelled away by the negative charge in the bottom triboelectric layer. The electrons will move from the bottom electrode to the top electrode through the external conductive path (state ii), until the two triboelectric layers are completely separated, and the charge reaches the equilibrium state (state iii). When the two triboelectric layers are close to each other again, the upper and lower triboelectric layers approach each other to generate a reverse internal electric field, and the electrons flow from the upper electrode to the lower electrode through the conductive path (state iv). When the upper and lower triboelectric layers are completely in contact, a cycle will be completed. With the continuous application and release of an external force, the PL-TENG will repeatedly complete the cycle shown in Figure 2. Finite

element simulation software was used to simulate the electrostatic field distribution under four different open-circuit conditions, and the results are shown in Figure 2b.

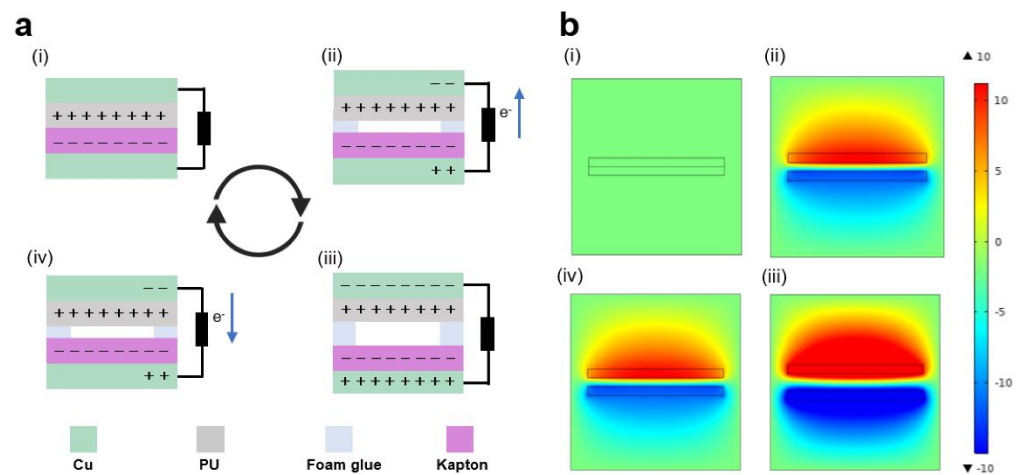


**Figure 2.** Working mechanism of the TENG (a) Working principle of the TENG. (i) The PL-TENG is compressed. (ii) The triboelectric layer of the PL-TENG gradually separates. (iii) The triboelectric layer of the PL-TENG is completely separated. (iv) The PL-TENG is compressed, and its triboelectric layer is gradually approached. (b) COMSOL software demonstrates the working principle of the PL-TENG. (i) the PL-TENG is compressed. (ii) The triboelectric layer of the PL-TENG gradually separates. (iii) The triboelectric layer of the PL-TENG is completely separated. (iv) Under an external force, the friction layer of the PL-TENG moves close again.

In order to accurately monitor the fast changes while playing wheelchair table tennis, the PL-TENG needs to transmit the movement data in real time. This allows the accurate integration and analysis of technical information. The PL-TENG output electric signal is the basis for analyzing the athlete's movement. An excellent signal response is fundamental as a motion monitoring tool. Considering the possible influence of external factors on the PL-TENG during movement, the performance of the PL-TENG was tested before the technical monitoring and analysis. A stepper motor was used to simulate the playing action at different pressures and frequencies. The equipment was fixed on the stepper motor with a transparent tape. The output performance of the equipment was tested by controlling the stepper motor to provide periodic contact separation. The distance and frequency of the stepper motor were adjusted to simulate the different states of an athlete in a competition. Figure 3a shows the output voltage at the same frequency under different pressures. When the pressure was 5 N, 10 N, 15 N, 20 N, 25 N, the output voltage was 0.36 V, 1.41 V, 2 V, and 2.7 V, respectively. The output voltage of the TENG increased significantly as the pressure increased. It responded well to changes in different pressures. Figure 3b shows the linear relationship between pressure and output voltage. It can be seen that there is a significant linear relationship between pressure and voltage; the Pearson correlation coefficient was 0.97, and the formula is:

$$V = 0.08 + 0.11 \times N \quad (1)$$

Since the movement of the gravity center causes pressure changes, the different voltages represent an athlete's different movement states and the body's control over the center of gravity. Coaches can accurately analyze an athlete's technical performance during training or competition according to the voltage signal emanating from the PL-TENG. Figure 3c shows the output voltage of the PL-TENG at different frequencies. When the frequency was 0.5 Hz, 1 Hz, 1.5 Hz, and 2 Hz, the output voltage was 1.2 V, 1.3 V, 1.2 V, 1.04 V, respectively. The results showed that the output voltage of the PL-TENG was stable at

different frequencies. Figure 3d shows the output voltage response at different frequencies, and the calculation formula is:

$$R\% = \frac{V_0 - V_i}{V_i} \times 100\% \quad (2)$$

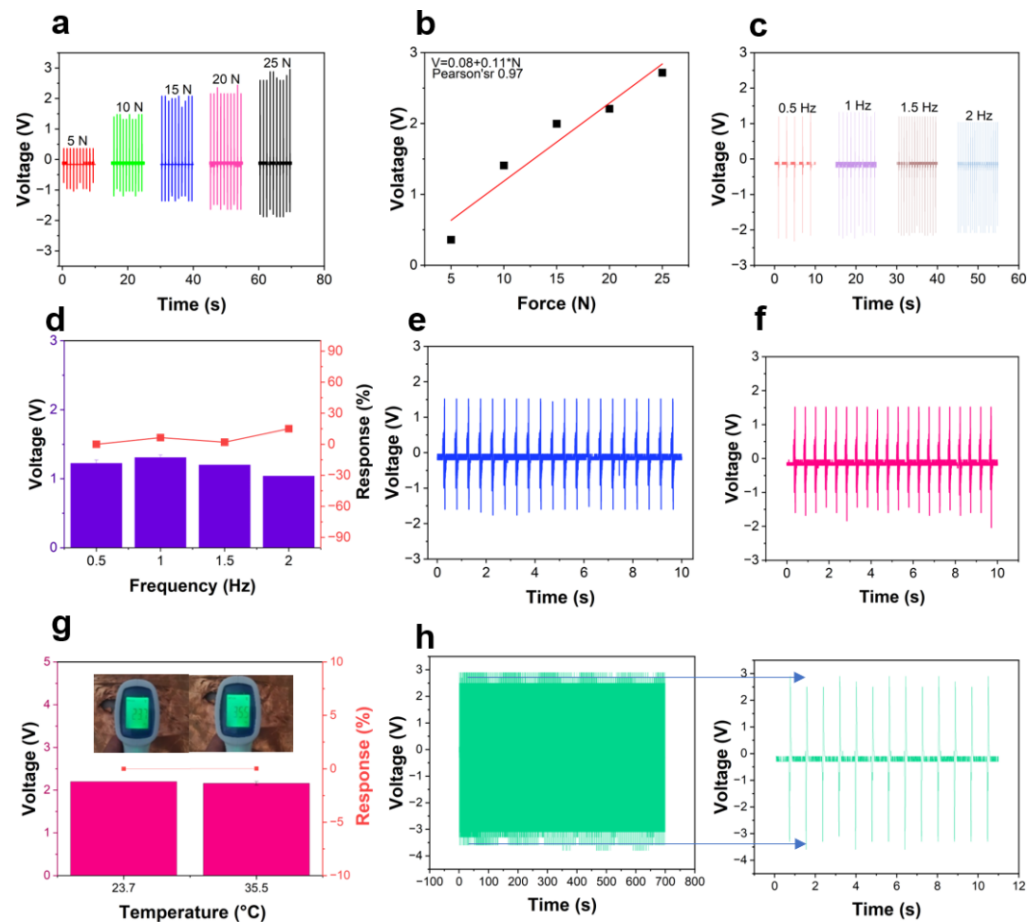


**Figure 3.** The output performance of the PL-TENG. (a) PL-TENG output voltage comparison under different pressures. (b) Linearity of the PL-TENG output voltage under different pressures. (c) PL-TENG output voltage comparison under different frequencies. (d) PL-TENG output voltage response under different frequencies. (e) PL-TENG output in dry conditions (voltage). (f) Output voltage of the PL-TENG after wetting. (g) Output voltage of the PL-TENG at different temperatures. (h) Durability test of the PL-TENG.

Here,  $V_0$  is the output voltage at 0.5 Hz, and  $V_i$  is the output voltage at other frequencies. Table tennis involves drastic movements. The metabolic rate of the human body is accelerated under continuous high-intensity exercise. Inevitably, for stabilizing the body temperature, the body will emit more heat and sweat during competition. The PL-TENG is in direct contact with the human body as it is fixed on it by adhesive tape. The temperature of the body and the sweat produced by the movement may affect the performance of the equipment.

The equipment was sealed during the experiments and applications. The PL-TENG output voltage before and after sweat-wetting at the same pressure and frequency, respectively, is shown in Figures 3e and 3f. The output voltage of the PL-TENG was 1.516 V before wetting and 1.516 V after wetting. The results showed that sweat had almost no effect on the output voltage of the PL-TENG. The effects of human body temperature changes should be considered. We performed output stability tests at different temperatures. Figure 3g shows the high stability of the PL-TENG output at different temperatures. It

proves that the PL-TENG can be used for wheelchair table tennis monitoring. The durability of the PL-TENG ensures a long-term monitoring. Figure 3h shows the durability of the PL-TENG. The results showed that the PL-TENG could still ensure a stable output after a long working time.

The PL-TENG can be applied to electrical energy harvesting. The energy generated during human movement can be collected and reused by the PL-TENG. The PL-TENG was installed using the circuit in Figure 4a. The 20 green LEDs in Figure 4b were lit by the tapping energy collected by the PL-TENG (Video S1). The electrical energy collected and stored by the PL-TENG can be used by small electronic devices. The current generated by the PL-TENG is AC. A rectifier bridge was installed in the circuit so that the AC current was converted to DC current to charge a capacitor of 4.7  $\mu\text{F}$ . After charging was completed, the switch in the circuit was turned on to supply power to small electronic devices (Figure S4). Figure 4c shows a schematic of the PL-TENG installed in the same circuit as the rectifier. The energy accumulated by the PL-TENG during human activities was used to power calculators and electronic watches, as shown in Figure 4d,e (Videos S2 and S3).

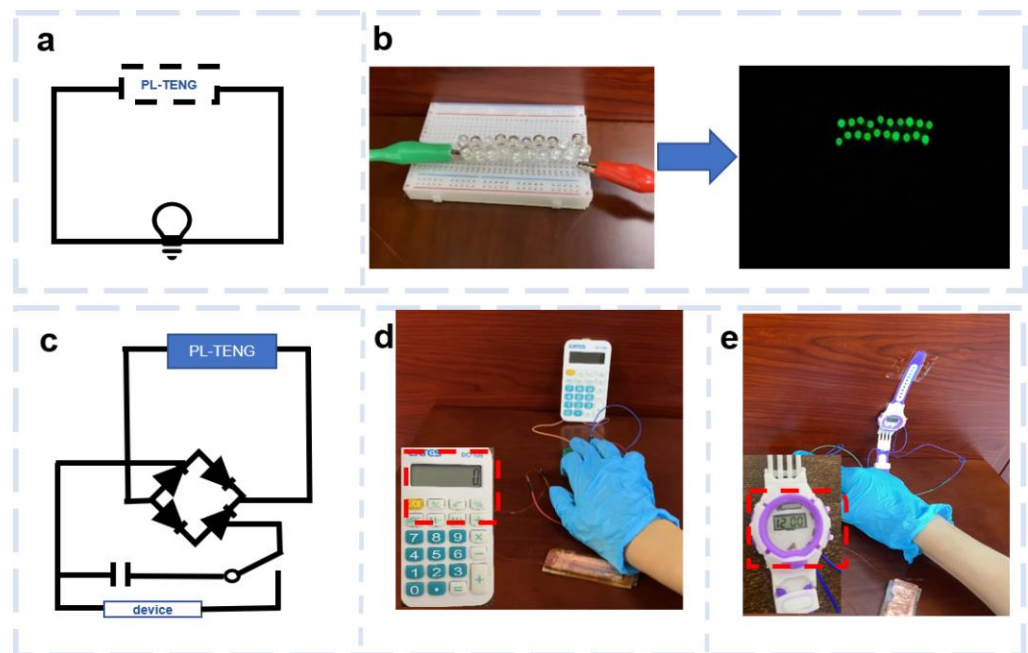


**Figure 4.** Application of the PL-TENG as a power supply. (a) Diagram of the PL-TENG lighting an LED circuit. (b) PL-TENG powering LEDs. (c) PL-TENG in the rectifier circuit. (d) PL-TENG as a calculator power supply. (e) PL-TENG as an electronic watch power supply.

Body control is important for both offense and defense in table tennis. Wheelchair table tennis athletes mainly rely on the torso to control the distance of the upper limbs to attack and defend. Reducing the movement of the wheelchair as much as possible will help athletes to make fast breaks and return to defense. An athlete's trunk control ability can be shown in the length of time necessary to complete a certain movement. A complete batting movement includes not only a ready position movement and a batting movement but also a body motion adjustment at the end of a stroke. Figure 5 shows the application of the PL-TENG in training. The PL-TENG was mounted on the seat of the wheelchair. The motion data were transmitted wirelessly to a computer (Figure S4) through an AD module and a Bluetooth module (Figure S5). Coaches can analyze the data on the computer to give specific instructions to athletes. Table tennis athletes face balls from different directions in a match. The athlete is required to constantly change the center of gravity to accommodate the changing direction of the ball. An athlete's body barycenter changes following the batting direction. As shown in Figure 5a, an athlete holding the racket in his right hand has his body barycenter tilted to the right when hitting a forehand. The barycenter is on the left

when hitting a backhand. Figure 5b shows the electric signal output of the R-PL-TENG on the center of gravity side of the athlete when the player hit a short ball three times with his forehand. The output voltage of the PL-TENG increased when the center of gravity of the athlete's body moved away from the central axis of the body along the direction of batting. Athletes need a great trunk control for balance and accuracy. Different signals can be produced by an athlete's performing three forehand shots, which would show that the athlete is not accurate enough [47] when batting balls in the same position. Athletes need to increase the number of practicing sessions [48]. Figure 5c shows the L-PL-TENG electrical signal output on the center of gravity side of an athlete hitting a backhand short ball three times. Comparing Figures 5b and 5c, it can be seen that the output voltage of the backhand shots was higher than that of the forehand shots, because the athlete needs more support strength to maintain his body balance when hitting a backhand short ball. In this case, compared to the ipsilateral support of the forehand, the torso adds a torsion motion. The trunk torsion force increases the batting power and also the difficulty of the torso to control the balance of the body. The athlete needs more strength control for the torso to overcome the inertia associated with the torsion. Therefore, a backhand short ball requires more trunk control than a forehand short ball. Strengthening the body core stability when playing a backhand can enhance the skill level of athletes. The athlete can judge the efficiency of a movement according to the completion time of a signal. The shorter the signal, the faster the action, which will allow the athlete to better prepare for the next attack. By comparing the completion times of the first signals in Figure 5b, c, it can be concluded that the backhand short ball of the athlete took a longer time. These data can be fed into the training exercise plan, to work on adding speed to the athlete's backhand. In a competition, the coach can put forward specific tactics for athletes according to the output voltage signals and the completion times of the signals. With more time to face the incoming ball, the athlete can hit the ball with more power thanks to the improved backhand. This will occur in a situation in which the player has to face a forehand attack with a counter-attack, making a quick return. When the opponent's ball is fast, the athlete can use a forehand shot to save time and adjust the movement. The output signal of the PL-TENG can be used to judge the attack and counter-attack movements of an athlete. The coach can analyze the athlete's performance according to the output signals. In order to explore whether the output of the TENG was affected by different arm haul distances, the output signals of the PL-TENG were compared by selecting shots with different arm haul distances. Figure 5d,e shows the output voltage comparison of the PL-TENG when hitting the ball with different arm haul angles. Figure 5d shows the influence of different arm haul distances of forehand shots on the output voltage of the PL-TENG. The arm haul distance with a shoulder abduction angle of about 45° and the arm haul distance with a shoulder abduction angle of about of 80° were compared [49]. The abduction angle of the shoulder affects the racket lead distance when hitting a forehand. A greater shoulder abduction angle for the same forehand shots will make the racket lead distance longer. Taking the central axis of the human body as the central axis of rotation, the length of the racket swing distance increases the moment arm, and the moment of inertia increases. The formula is as follows:

$$I = mr^2 \quad (3)$$

where  $r$  is the distance from the table tennis racket to the athlete's center axis, and  $m$  refers to the mass of the athlete's body. As the moment of inertia increases, more force is required from the torso to maintain balance at the end of the movement. The PL-TENG showed an increase in output voltage. During wheelchair table tennis backhand shots achieved mainly through the wheelchair movement, the athlete torsion rotates, followed by shoulder joint adduction and internal rotation. The wheelchair movement should be minimized during the game to prevent passive situations. Figure 5e shows the signal output of the PL-TENG backhand shot from different angles. An athlete's torsional angle and shoulder joint rotation and adduction are important influencing factors in hitting backhands. The functional axial rotation angle of the lumbar spine is between 2° and 7° [50]. A long-haul

backhand shot obviously produces a higher electrical signal. Because of the limitation of the angle of motion of the joint, athletes usually increase the range of motion by lateral bending of the pelvis. This also increases the time to complete the overall movement. The complexity of the body motion involves a high number of muscle groups. The more complex the athlete’s movement, the better the muscle control ability the athlete requires. By comparing the completion time of two identical movements it is possible to estimate the muscle control ability of an athlete. The data in Figure 5e prove that the athlete had optimal control over the muscles. The PL-TENG can be applied to monitor the motion data of wheelchair table tennis athletes. It captures and visualizes subtle changes in an athlete’s body movements while playing. Coaches and athletes can more easily identify deficiencies during movement by using sensing devices with the PL-TENG. Sensing equipment with the PL-TENG provides the support of scientific and intuitive for athletes’ technical training.

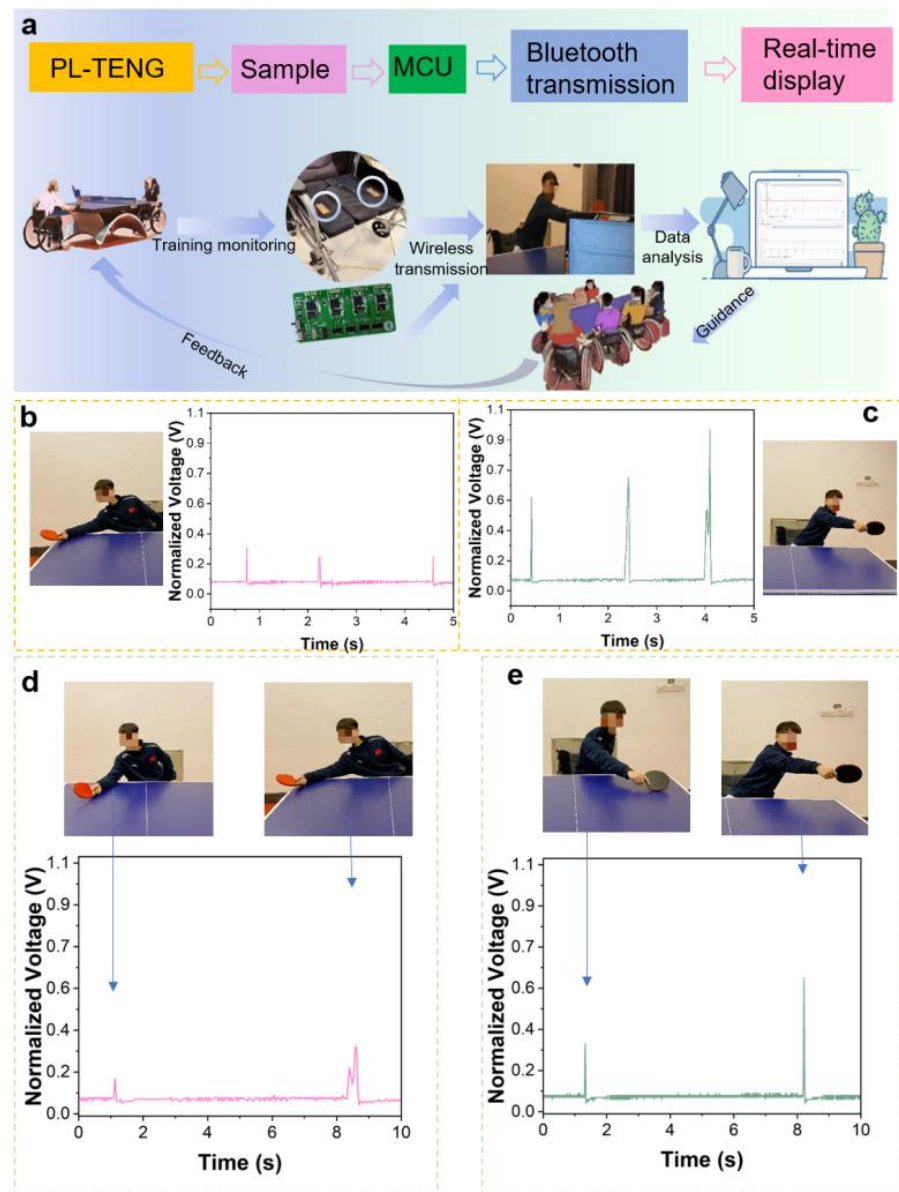


**Figure 5.** (a) Using the PL-TENG wireless transmission of motion data and guidance analysis. (b) Output voltage signals of three forehand short balls. (c) Output voltage signals of three backhand short balls. (d) Comparison of the PL-TENG output voltages when hitting forehand balls at different distances. (e) Comparison of the PL-TENG output voltage when hitting backhand balls at different distances.

#### 4. Conclusions

In conclusion, a new portable and comfortable TENG was developed for motion monitoring. A PU film and a Kapton film constitute the triboelectric layer, and the foam glue is combined as the support layer. This avoids expensive and time-consuming processing, which makes the PL-TENG easy to manufacture and low-cost. The PL-TENG powers microelectronics by harvesting the energy of movement. The use of the PL-TENG can reduce the environmental pollution caused by conventional batteries. Sensing equipment with the PL-TENG can be used while playing sports in place of traditional motion monitoring equipment. The PL-TENG was developed to solve the problem of inflexible motion monitoring devices. It provides a low-cost solution for real-time motion monitoring. It opens new perspectives for sports intelligence.

**Supplementary Materials:** The following supporting information can be downloaded at: <https://www.mdpi.com/article/10.3390/electronics11244189/s1>, Figure S1: PL-TENG mounted on a wheelchair; Figure S2: Working diagram of the PL-TENG simulated by a stepper motor; Figure S3: Information about the rectifier diode and the capacitor used; Figure S4: The PL-TENG wirelessly transmits motion signals through Bluetooth; Figure S5: Bluetooth module used in sensing, Video S1: Testing the energy harvesting performance of the PL-TENG by lighting LEDs; Video S2: Testing the PL-TENG energy harvesting performance by powering a calculator; Video S3: Testing the energy harvesting performance of the PL-TENG by powering an electronic watch.

**Author Contributions:** Conceptualization, methodology, software, validation, formal analysis, investigation, X.Z.; resources, data curation, writing original, M.Z.; draft preparation, X.W.; writing review and editing, visualization, supervision, Y.Z.; project administration, funding acquisition, C.J. All authors have read and agreed to the published version of the manuscript.

**Funding:** This research received no external funding.

**Data Availability Statement:** The data presented in this study are available in Supplementary Materials.

**Acknowledgments:** The authors would like to thank the collaboration of all volunteers who participated in the data collection.

**Conflicts of Interest:** The authors declare no conflict of interest.

#### References

1. Blauwet, C.; Willick, S.E. The Paralympic Movement: Using Sports to Promote Health, Disability Rights, and Social Integration for Athletes with Disabilities. *Pm R* **2012**, *4*, 851–856. [[CrossRef](#)] [[PubMed](#)]
2. Mauerberg-de Castro, E.; Campbell, D.F.; Tavares, C.P. The global reality of the Paralympic Movement: Challenges and opportunities in disability sports. *Mot. Rev. Educ. Fis.* **2016**, *22*, 111–123.
3. Nagel-Albustin, K.; Crevenna, R. Table tennis for the disabled. *Phys. Med. Rehab. Kurortmed.* **2008**, *18*, 150–154. [[CrossRef](#)]
4. Duvall, J.; Gebrosky, B.; Ruffing, J.; Anderson, A.; Ong, S.S.; McDonough, R.; Cooper, R.A. Design of an adjustable wheelchair for table tennis participation. *Disabil. Rehabil.-Assist. Technol.* **2021**, *16*, 425–431. [[CrossRef](#)] [[PubMed](#)]
5. Xiao, N.; Yu, W.; Han, X. Wearable heart rate monitoring intelligent sports bracelet based on Internet of things. *Measurement* **2020**, *164*, 108102. [[CrossRef](#)]
6. Cao, L.N.Y.; Xu, Z.; Wang, Z.L. Application of Triboelectric Nanogenerator in Fluid Dynamics Sensing: Past and Future. *Nanomaterial* **2022**, *12*, 3261. [[CrossRef](#)] [[PubMed](#)]
7. Cao, X.; Jie, Y.; Wang, N.; Wang, Z.L. Triboelectric Nanogenerators Driven Self-Powered Electrochemical Processes for Energy and Environmental Science. *Adv. Energy Mater.* **2016**, *6*, 1600665. [[CrossRef](#)]
8. Nguyen, Q.-T.; Ahn, K.-K.K. Fluid-Based Triboelectric Nanogenerators: A Review of Current Status and Applications. *Int. J. Precis. Eng. Manuf. Green Technol.* **2021**, *8*, 1043–1060. [[CrossRef](#)]
9. Wang, Y.; Yang, Y.; Wang, Z.L. Triboelectric nanogenerators as flexible power sources. *NPJ Flex. Electron.* **2017**, *1*, 10. [[CrossRef](#)]
10. Wu, Z.; Cheng, T.; Wang, Z.L. Self-Powered Sensors and Systems Based on Nanogenerators. *Sensors* **2020**, *20*, 2925. [[CrossRef](#)]
11. Cai, J.; Zhang, Z. A Spring Structure Triboelectric Nanogenerator for Human Gait Monitoring System. *Nano* **2022**, *17*, 2250001. [[CrossRef](#)]
12. Jin, L.; Tao, J.; Bao, R.; Sun, L.; Pan, C. Self-powered Real-time Movement Monitoring Sensor Using Triboelectric Nanogenerator Technology. *Sci. Rep.* **2017**, *7*, 10521. [[CrossRef](#)] [[PubMed](#)]
13. Dai, S.; Li, X.; Jiang, C.; Zhang, Q.; Peng, B.; Ping, J.; Ying, Y. Omnidirectional wind energy harvester for self-powered agro-environmental information sensing. *Nano Energy* **2022**, *91*, 106686. [[CrossRef](#)]

14. Guo, H.; Wan, J.; Wang, H.; Wu, H.; Xu, C.; Miao, L.; Han, M.; Zhang, H. Self-Powered Intelligent Human-Machine Interaction for Handwriting Recognition. *Research* **2021**, *2021*, 4689869. [[CrossRef](#)] [[PubMed](#)]
15. Jiang, M.; Lu, Y.; Zhu, Z.; Jia, W. Advances in Smart Sensing and Medical Electronics by Self-Powered Sensors Based on Triboelectric Nanogenerators. *Micromachines* **2021**, *12*, 698. [[CrossRef](#)]
16. Liu, S.; Yuan, G.; Zhang, Y.; Xie, L.; Shen, Q.; Lei, H.; Wen, Z.; Sun, X. A Self-Powered Gas Sensor Based on Coupling Triboelectric Screening and Impedance Matching Effects. *Adv. Mater. Technol.* **2021**, *6*, 2100310. [[CrossRef](#)]
17. Yu, A.; Chen, L.; Chen, X.; Zhang, A.; Fan, F.; Zhan, Y.; Wang, Z.L. Triboelectric sensor as self-powered signal reader for scanning probe surface topography imaging. *Nanotechnology* **2015**, *26*, 165501. [[CrossRef](#)]
18. Zhao, T.; Fu, Y.; Sun, C.; Zhao, X.; Jiao, C.; Du, A.; Wang, Q.; Mao, Y.; Liu, B. Wearable biosensors for real-time sweat analysis and body motion capture based on stretchable fiber-based triboelectric nanogenerators. *Biosens. Bioelectron.* **2022**, *205*, 114115. [[CrossRef](#)]
19. Bai, Y.; Xu, L.; He, C.; Zhu, L.; Yang, X.; Jiang, T.; Nie, J.; Zhong, W.; Wang, Z.L. High-performance triboelectric nanogenerators for self-powered, in-situ and real-time water quality mapping. *Nano Energy* **2019**, *66*, 104117. [[CrossRef](#)]
20. Jia, C.J.; Zhu, Y.S.; Sun, F.X.; Wen, Y.Z.; Wang, Q.; Li, Y.; Mao, Y.P.; Zhao, C.L. Gas-Supported Triboelectric Nanogenerator Based on In Situ Gap-Generation Method for Biomechanical Energy Harvesting and Wearable Motion Monitoring. *Sustainability-basel* **2022**, *14*, 14422. [[CrossRef](#)]
21. Cho, H.; Kim, I.; Park, J.; Kim, D. A waterwheel hybrid generator with disk triboelectric nanogenerator and electromagnetic generator as a power source for an electrocoagulation system. *Nano Energy* **2022**, *95*, 107048. [[CrossRef](#)]
22. Gao, S.; Chen, Y.; Su, J.; Wang, M.; Wei, X.; Jiang, T.; Wang, Z.L. Triboelectric Nanogenerator Powered Electrochemical Degradation of Organic Pollutant Using Pt-Free Carbon Materials. *ACS Nano* **2017**, *11*, 3965–3972. [[CrossRef](#)] [[PubMed](#)]
23. Han, G.; Wu, B.; Pu, Y. High output triboelectric nanogenerator based on scotch tape for self-powered flexible electrics. *Mater. Technol.* **2022**, *37*, 224–229. [[CrossRef](#)]
24. He, C.; Wang, Z.L. Triboelectric nanogenerator as a new technology for effective PM2.5 removing with zero ozone emission. *Prog. Nat. Sci.-Mater. Int.* **2018**, *28*, 99–112. [[CrossRef](#)]
25. Liu, D.; Chen, B.; An, J.; Li, C.; Liu, G.; Shao, J.; Tang, W.; Zhang, C.; Wang, Z.L. Wind-driven self-powered wireless environmental sensors for Internet of Things at long distance. *Nano Energy* **2020**, *73*, 104819. [[CrossRef](#)]
26. Ma, M.; Kang, Z.; Liao, Q.; Zhang, Q.; Gao, F.; Zhao, X.; Zhang, Z.; Zhang, Y. Development, applications, and future directions of triboelectric nanogenerators. *Nano Res.* **2018**, *11*, 2951–2969. [[CrossRef](#)]
27. Pang, Y.; Zhu, X.; Lee, C.; Liu, S. Triboelectric nanogenerator as next-generation self-powered sensor for cooperative vehicle-infrastructure system. *Nano Energy* **2022**, *97*, 107219. [[CrossRef](#)]
28. Qian, C.; Li, L.; Gao, M.; Yang, H.; Cai, Z.; Chen, B.; Xiang, Z.; Zhang, Z.; Song, Y. All-printed 3D hierarchically structured cellulose aerogel based triboelectric nanogenerator for multi-functional sensors. *Nano Energy* **2019**, *63*, 103885. [[CrossRef](#)]
29. Saqib, Q.M.; Shaikat, R.A.; Khan, M.U.; Chougale, M.; Bae, J. Biowaste Peanut Shell Powder-Based Triboelectric Nanogenerator for Biomechanical Energy Scavenging and Sustainably Powering Electronic Supplies. *ACS Appl. Electron. Mater.* **2020**, *2*, 3953–3963. [[CrossRef](#)]
30. Tian, J.; Wang, F.; Ding, Y.; Lei, R.; Shi, Y.; Tao, X.; Li, S.; Yang, Y.; Chen, X. Self-Powered Room-Temperature Ethanol Sensor Based on Brush-Shaped Triboelectric Nanogenerator. *Research* **2021**, *2021*, 8564780. [[CrossRef](#)]
31. Wang, X.; Yin, Y.; Yi, F.; Dai, K.; Niu, S.; Han, Y.; Zhang, Y.; You, Z. Bioinspired stretchable triboelectric nanogenerator as energy-harvesting skin for self-powered electronics. *Nano Energy* **2017**, *39*, 429–436. [[CrossRef](#)]
32. Xia, K.; Zhu, Z.; Fu, J.; Li, Y.; Chi, Y.; Zhang, H.; Du, C.; Xu, Z. A triboelectric nanogenerator based on waste tea leaves and packaging bags for powering electronic office supplies and behavior monitoring. *Nano Energy* **2019**, *60*, 61–71. [[CrossRef](#)]
33. Xu, L.; Xu, L.; Luo, J.; Yan, Y.; Jia, B.-E.; Yang, X.; Gao, Y.; Wang, Z.L. Hybrid All-in-One Power Source Based on High-Performance Spherical Triboelectric Nanogenerators for Harvesting Environmental Energy. *Adv. Energy Mater.* **2020**, *10*, 2001669. [[CrossRef](#)]
34. Yu, X.; Ge, J.; Wang, Z.; Wang, J.; Zhao, D.; Wang, Z.L.; Cheng, T. High-performance triboelectric nanogenerator with synchronization mechanism by charge handling. *Energy Convers. Manag.* **2022**, *263*, 115655. [[CrossRef](#)]
35. Yuan, H.; Yu, H.; Liu, X.; Zhao, H.; Zhang, Y.; Xi, Z.; Zhang, Q.; Liu, L.; Lin, Y.; Pan, X.; et al. A High-Performance Coniform Helmholtz Resonator-Based Triboelectric Nanogenerator for Acoustic Energy Harvesting. *Nanomaterials* **2021**, *11*, 3431. [[CrossRef](#)]
36. Yun, Y.; Jang, S.; Cho, S.; Lee, S.H.; Hwang, H.J.; Choi, D. Exo-shoe triboelectric nanogenerator: Toward high-performance wearable biomechanical energy harvester. *Nano Energy* **2021**, *80*, 105525. [[CrossRef](#)]
37. Sun, F.; Zhu, Y.; Jia, C.; Ouyang, B.; Zhao, T.; Li, C.; Ba, N.; Li, X.; Chen, S.; Che, T.; et al. A Flexible Lightweight Triboelectric Nanogenerator for Protector and Scoring System in Taekwondo Competition Monitoring. *Electronics* **2022**, *11*, 1306. [[CrossRef](#)]
38. Ma, X.; Liu, X.; Li, X.; Ma, Y. Light-Weight, Self-Powered Sensor Based on Triboelectric Nanogenerator for Big Data Analytics in Sports. *Electronics* **2021**, *10*, 2322. [[CrossRef](#)]
39. Ba, Y.-Y.; Bao, J.-F.; Deng, H.-T.; Wang, Z.-Y.; Li, X.-W.; Gong, T.; Huang, W.; Zhang, X.-S. Single-Layer Triboelectric Nanogenerators Based on Ion-Doped Natural Nanofibrils. *ACS Appl. Mater. Interfaces* **2020**, *12*, 42859–42867. [[CrossRef](#)]
40. Dong, K.; Deng, J.; Ding, W.; Wang, A.C.; Wang, P.; Cheng, C.; Wang, Y.-C.; Jin, L.; Gu, B.; Sun, B.; et al. Versatile Core-Sheath Yarn for Sustainable Biomechanical Energy Harvesting and Real-Time Human-Interactive Sensing. *Adv. Energy Mater.* **2018**, *8*, 1801114. [[CrossRef](#)]

41. Zhang, H.; Wang, H.; Zhang, J.; Zhang, Z.; Yu, Y.; Luo, J.; Dong, S. A novel rhombic-shaped paper-based triboelectric nanogenerator for harvesting energy from environmental vibration. *Sens. Actuator A Phys.* **2020**, *302*, 111806. [[CrossRef](#)]
42. Moon, H.-B.; Park, S.-J.; Kim, A.-C.; Jang, J.-H. Characteristics of upper limb muscular strength in male wheelchair tennis players. *J. Exerc. Rehabil.* **2013**, *9*, 375–380. [[CrossRef](#)] [[PubMed](#)]
43. Hu, J.; Pu, X.; Yang, H.; Zeng, Q.; Tang, Q.; Zhang, D.; Hu, C.; Xi, Y. A flutter-effect-based triboelectric nanogenerator for breeze energy collection from arbitrary directions and self-powered wind speed sensor. *Nano Res.* **2019**, *12*, 3018–3023. [[CrossRef](#)]
44. Zhang, J.; Xu, Q.; Gan, Y.; Sun, F.; Sun, Z. A Lightweight Sensitive Triboelectric Nanogenerator Sensor for Monitoring Loop Drive Technology in Table Tennis Training. *Electronics* **2022**, *11*, 3212. [[CrossRef](#)]
45. Wu, Y.; Luo, Y.; Qu, J.; Daoud, W.A.; Qi, T. Liquid single-electrode triboelectric nanogenerator based on graphene oxide dispersion for wearable electronics. *Nano Energy* **2019**, *64*, 103948. [[CrossRef](#)]
46. Srither, S.R.; Rao, D.S.S.; Prasad, S.K. Triboelectric Nanogenerator Based on Biocompatible and Easily Available Polymer Films. *Chemistryselect* **2018**, *3*, 5055–5061. [[CrossRef](#)]
47. Xia, R.; Dai, B.; Fu, W.; Gu, N.; Wu, Y. Kinematic Comparisons of the Shakehand and Penhold Grips in Table Tennis Forehand and Backhand Strokes when Returning Topspin and Backspin Balls. *J. Sports Sci. Med.* **2020**, *19*, 637–644.
48. Bankosz, Z.; Winiarski, S. The kinematics of table tennis racquet: Differences between topspin strokes. *J. Sports Med. Phys. Fit.* **2017**, *57*, 202–213. [[CrossRef](#)]
49. Doğan, M.; Koçak, M.; Onursal Kılınc, Ö.; Ayvat, F.; Sütçü, G.; Ayvat, E.; Kılınc, M.; Ünver, Ö.; Aksu Yıldırım, S. Functional range of motion in the upper extremity and trunk joints: Nine functional everyday tasks with inertial sensors. *Gait Posture* **2019**, *70*, 141–147. [[CrossRef](#)]
50. Miyachi, R.; Sano, A.; Tanaka, N.; Tamai, M.; Miyazaki, J. Measuring Lumbar Motion Angle with a Small Accelerometer: A Reliability Study. *J. Chiropr. Med.* **2022**, *21*, 32–38. [[CrossRef](#)]